Wnt5a signaling promotes apical and basolateral polarization of single epithelial cells

Hidetoshi Gon[a,b], Katsumi Fumoto[a], Yonson Ku[b], Shinji Matsumoto[a], and Akira Kikuchi[a]

[a]Department of Molecular Biology and Biochemistry, Graduate School of Medicine, Osaka University, 2-2 Yamadaoka, Suita, Osaka 565-0871, Japan; [b]Division of Hepato-Biliary-Pancreatic Surgery, Department of Surgery, Kobe University Graduate School of Medicine, 7-5-1 Kusunoki-cho, Chuo-ku, Kobe 650-0017, Japan

ABSTRACT Single epithelial-derived tumor cells have been shown to induce apical and basolateral (AB) polarity by expression of polarization-related proteins. However, physiological cues and molecular mechanisms for AB polarization of single normal epithelial cells are unclear. When intestinal epithelial cells 6 (IEC6 cells) were seeded on basement membrane proteins (Matrigel), single cells formed an F-actin cap on the upper cell surface, where apical markers accumulated, and a basolateral marker was localized to the rest of the cell surface region, in a Wnt5a signaling–dependent manner. However, these phenotypes were not induced by type I collagen. Rac1 activity in the noncap region was higher than that in the cap region, whereas Rho activity increased toward the cap region. Wnt5a signaling activated and inhibited Rac1 and RhoA, respectively, independently through Tiam1 and p190RhoGAP-A, which formed a tertiary complex with Dishevelled. Furthermore, Wnt5a signaling through Rac1 and RhoA was required for cystogenesis of IEC6 cells. These results suggest that Wnt5a promotes the AB polarization of IEC6 cells through regulation of Rac and Rho activities in a manner dependent on adhesion to specific extracellular matrix proteins.

INTRODUCTION

Cell polarity results from a vectorial axis that directs the internal organization of a cell and is observed in most differentiated cell types of eukaryotes and in unicellular organisms such as yeast (Bryant and Mostov, 2008; Berzat and Hall, 2010). Epithelial cells are organized into multicellular sheets of tubules that form distinct apical and basolateral compartments, which are divided by tight junctions (Baum and Georgiou, 2011). The apical membrane oriented toward the free space is morphologically, biochemically, and physiologically distinct from the basolateral membrane. Cultured epithelial cells

have been conventionally grown on glass or plastic, which provides a strong cue for cells to orient the apical surface away from the support. As a physiological cue, the orientation of polarity depends on the interaction of cells with the extracellular matrix (ECM). Therefore, to study epithelial polarity, epithelial cells must be grown on a filter two dimensionally or in the ECM three dimensionally. In vitro experiments using cultured cells revealed that tight junctions are not always necessary for the formation of apical and basolateral (AB) polarity in epithelial cells (Umeda et al., 2006; Vega-Salas et al., 1987), but that cell-to-cell junctions are involved in the formation of distinct apical and basolateral domains (Grindstaff et al., 1998; Suzuki et al., 2002; Baum and Georgiou, 2011). To understand the mechanism by which the ECM, especially basement membrane proteins, defines AB polarity, single cells should be cultured around the circumference surrounded by basement membrane proteins.

It has been reported that single epithelial cells establish polarity with brush border formation, which is similar to AB polarity, in a cell-autonomous manner in the absence of cell-to-cell and cell-to-substrate adhesion (Baas et al., 2004). In this model, the LKB1/STRAD/MO25 complex induces enrichment of phosphatidylinositol-4,5-bisphosphates (PIP2) in the apical membrane, where phospholipase D1 is recruited and produces phosphatidic acid, which also binds to the guanine nucleotide exchange factor (GEF) PDZGEF. Subsequently, a

Abbreviations used: AB, apical and basolateral; Dvl, Dishevelled; ECM, extracellular matrix; FAK, focal adhesion kinase; FRET, fluorescence resonance energy transfer; GAP, GTPase-activating protein; GEF, guanine nucleotide exchange factor; GFP, green fluorescent protein; IEC6, intestinal epithelial cell 6; pEzrin, phosphorylated ezrin; siRNA, small interfering RNA; TFP, teal fluorescent protein.
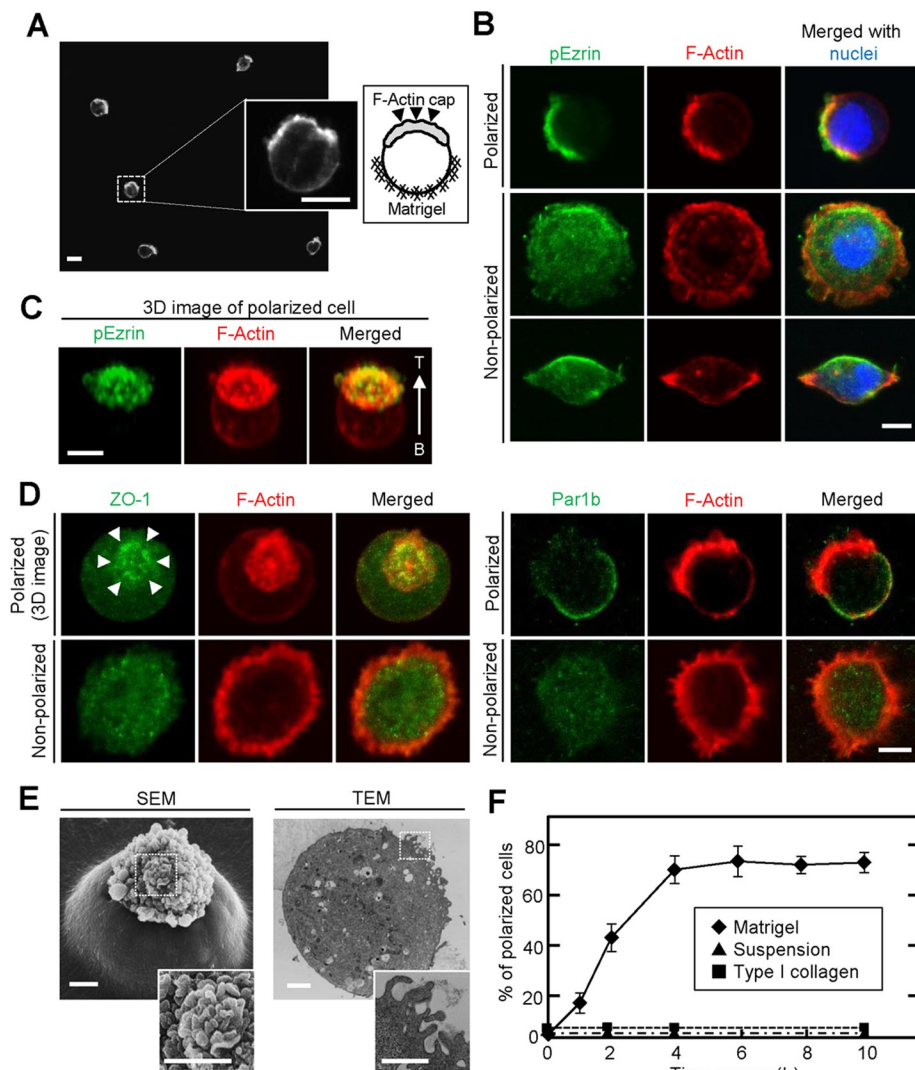
FIGURE 1: IEC6 cells show a polarized cell shape at the single-cell level in a Matrigel-dependent manner. (A) IEC6 cells cultured on Matrigel for 8 h were stained for F-actin. Left and right inserts, enlarged view and schema, respectively, of the area within the dashed box. (B) IEC6 cells were plated on Matrigel for 2 h and stained for pEzrin (green), F-actin (red), and DRAQ5 (blue). Top, a typical polarized cell; bottom, unpolarized cells. (C) Three-dimensional image of typical polarized IEC6 cells generated from an image stack. T, top; B, bottom. (D) IEC6 cells were plated on Matrigel and stained for ZO-1 (green, left) or Par1b (green, right) and F-actin (red). (E) The presence of microvillus structures on top of single IEC6 cells was observed by SEM (left) and TEM (right). Bottom, enlargement of images within the dashed boxes, indicating the apical surface. (F) IEC6 cells were suspended in growth medium (▲) or plated on Matrigel (◆) or type I collagen gel (■) for indicated time periods. Polarized cells among at least 100 cells were counted at indicated time points and expressed as the percentage of polarized cells. Results are means ± SD from three independent experiments. Scale bars, 10 μm (A), 5 μm (B–D), 2 μm (E).

β-catenin–dependent and –independent pathways (Kikuchi et al., 2011). In the former pathway, β-catenin mediates the signal to the nucleus, where gene expression is regulated. The latter pathway is believed to regulate the cytoskeleton mainly through the activation of protein kinases and small G proteins, thereby coordinating cell migration and polarity. Genetic studies showed that the β-catenin–independent pathway regulates planar cell polarity (PCP), which entails rearrangements of the cytoskeleton oriented at right angles to the AB polarity in the epithelium (Veeman et al., 2003). Wnt5a is a representative ligand that activates the β-catenin–independent pathway and is involved in PCP in various species (Kikuchi et al., 2012). In previous work, we showed that Wnt5a signaling is required for cell-to-substrate adhesion, migration through the focal adhesion turnover, and formation of front–rear polarity (Kurayoshi et al., 2006; Yamamoto et al., 2009; Matsumoto et al., 2010). However, it was not known whether Wnt5a signaling is involved in AB polarization. In this study, we establish that rat normal intestinal epithelial cells orient AB polarity at a single-cell level in an adhesion-dependent manner to Matrigel, which contains specific basement membrane proteins, including laminin, nidogen, and type IV collagen, and show that Wnt5a signaling promotes polarization by regulating the balance between the activities of Rac and Rho.

RESULTS

Intestinal epithelial cells show polarized cell shape at the single-cell level

To examine whether epithelial cells are polarized cell-autonomously without cell-to-cell adhesion, we seeded single cells of various epithelial cell lines, including intestinal epithelial cells 6 (IEC6 cells), mouse mammary gland epithelial cells (EpH4 cells), and canine kidney epithelial cells (MDCK cells), sparsely on thick Matrigel, followed by incubation with culture medium containing 2% Matrigel. A number of IEC6 cells showed a spherical shape with an F-actin cap on the opposite side to the Matrigel (Figure 1A),

signaling cascade, including Rap2A, TNIK, and MST4, forms the brush border through the phosphorylation of ezrin at the plasma membrane (Gloerich et al., 2012). However, these studies were done using a colon cancer cell line, Ls174T, in which LKB1, a tumor suppressor gene product, is overexpressed and activated. Therefore it is still unclear whether normal single epithelial cells orient AB polarization depending on only the ECM and which endogenous signaling is involved in polarization.

Wnt proteins constitute a large family of cysteine-rich secreted ligands that are essential for a wide array of developmental and physiological processes (Logan and Nusse, 2004). Wnt activates the

but EpH4 and MDCK cells did not show these phenotypes (Supplemental Figure S1, A and B).

Phosphorylated ezrin (pEzrin), an apical marker, was strikingly colocalized with F-actin in these IEC6 cells (Figure 1, B and C). In addition, other apical markers—protein kinase Cζ (PKCζ) and PIP2—were also observed with F-actin (Supplemental Figure S1C), whereas ZO-1, a tight junction marker, accumulated around the F-actin cap, and Par1b, a basolateral marker, was localized to the areas other than the F-actin cap (Figure 1D), indicating that these cells developed AB polarity. Scanning electron microscopy (SEM) and transmission electron microscopy (TEM) revealed that the lower half of a
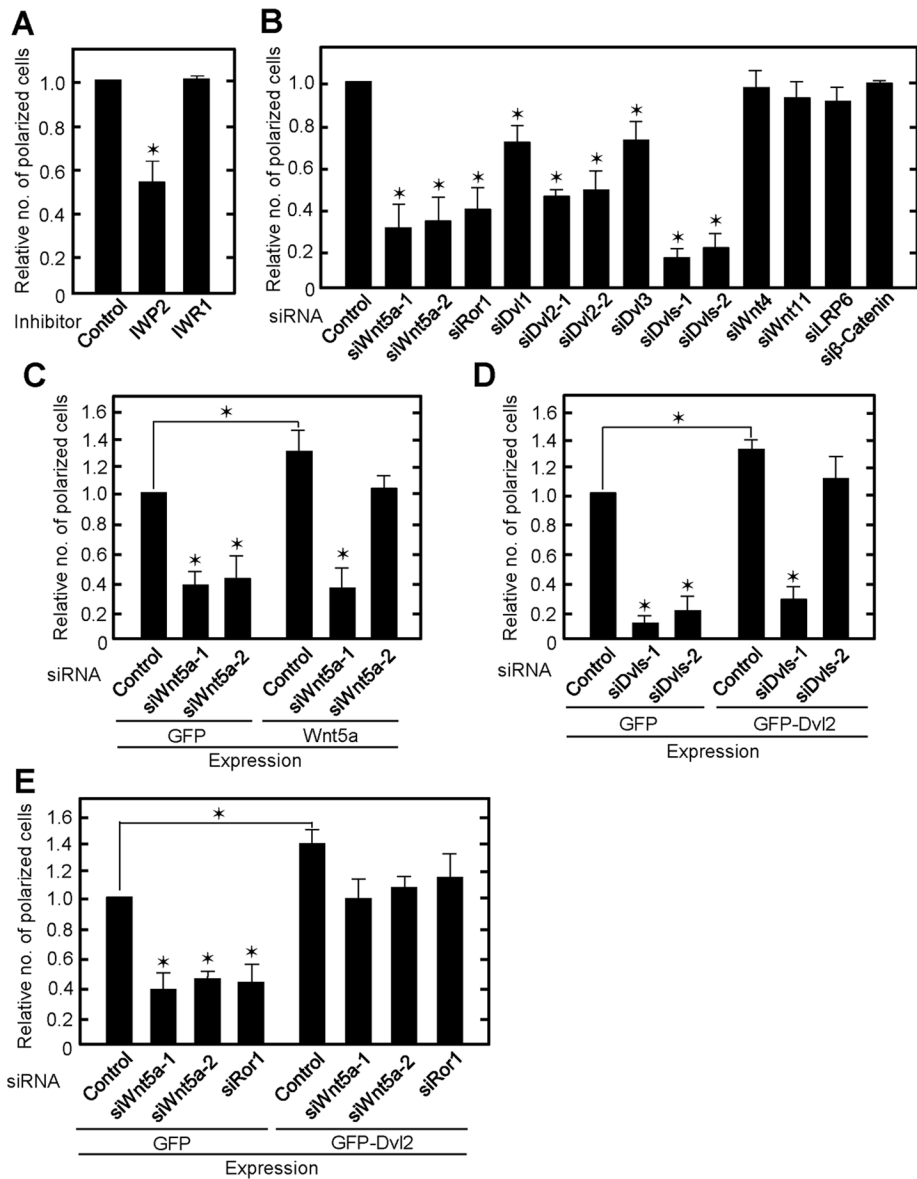
FIGURE 2: Wnt5a signaling is required for single-cell polarization of IEC6 cells. (A) IEC6 cells treated with IWP2 or IWR1 for 24 h were plated on Matrigel for 2 h. Polarized cells among total cells were counted, and the percentage of polarized cells was calculated. The ratios of the percentages of polarized cells were compared with controls. (B) IEC6 cells transfected with indicated siRNA were plated on Matrigel. siDvls-1, a mixture of siDvl1, siDvl2-1, and siDvl3; siDvls-2, a mixture of siDvl1, siDvl2-2, and siDvl3. (C) GFP- or Wnt5a-expressing IEC6 cells were transfected with Wnt5a siRNA and plated on Matrigel. (D) GFP- or GFP-Dvl2-expressing IEC6 cells were transfected with Dvls siRNA and plated on Matrigel. (E) GFP- or GFP-Dvl2-expressing IEC6 cells were transfected with Wnt5a or Ror1 siRNA. Results are means ± SD from three independent experiments. *$p < 0.01$.

then a polarized F-actin cap emerged after massive reorganization of the actin cytoskeleton (Supplemental Figure S1D).

The Rap2-TNIK-Mst4 axis induces brush border formation through the phosphorylation of Ezrin in single Ls174T cells (Gloerich et al., 2012). Because the knockdown of Mst4 did not affect single-cell polarization of IEC6 cells (Supplemental Figure S1E), other mechanisms must exist to induce this phenomenon. IEC6 cells showed no sign of polarization when they were cultured in suspension or seeded on thick type I collagen gel (Figure 1F and Supplemental Figure S1F). Furthermore, IEC6 cells cultured two dimensionally on Matrigel-coated dishes just spread and could not form F-actin cap (Supplemental Figure S1G). Therefore, in addition to the contact with Matrigel components, environmental cues, such as the stiffness of thick ECM matrix, might be involved in the single-cell AB polarization of IEC6 cells.

Wnt5a signaling is involved in single-cell polarization

We showed previously that Wnt5a signaling is necessary for HeLa and Vero cells to bind to the ECM and determine front–rear polarity (Matsumoto et al., 2010). This prompted us to test the effects of Wnt signaling on ECM-dependent single-cell polarization. IWP2 inhibits Wnt secretion, resulting in the suppression of both the β-catenin–dependent and –independent pathways, and IWR1 stabilizes Axin1, thereby suppressing the β-catenin–dependent pathway (Chen et al., 2009). Single-cell polarization was suppressed by IWP2 but not IWR1 (Figure 2A), suggesting that the β-catenin–independent but not the β-catenin–dependent pathway is required. Consistently, knockdown of LRP6 and β-catenin, which are major components of the β-catenin–dependent pathway, did not affect single-cell polarization (Figure 2B and Supplemental Figure S2A).

In IEC6 cells, mRNAs of Wnt4, Wnt5a, and Wnt11 were expressed at higher levels than those of Wnt2b, Wnt3, Wnt5b, Wnt6, Wnt7a, Wnt7b, and Wnt9b (Supplemental Figure S2B). Endogenous Wnt5a protein was indeed detected in IEC6 cells, and its expression level was higher than in EpH4 and MDCK cells (Supplemental Figure S2C). Polarization was significantly reduced in Wnt5a-depleted IEC6 cells, in which Wnt5a was decreased by small interfering RNA (siRNA) against the coding region (siWnt5a-1) and the 3′-untranslated region (siWnt5a-2; Figure 2B and Supplemental Figure S2D). However, knockdown of Wnt4 or Wnt11 did not affect single-cell polarization (Figure 2B and Supplemental Figure S2E). Expression of Wnt5a restored the phenotype induced by siWnt5a-2 but not that induced by siWnt5a-1 (Figure 2C and Supplemental Figure S2D), thereby excluding siRNA off-target effects. Knockdown of Ror1, a

polarized cell was embedded in the Matrigel and the upper half had clustered microvillus-like structures on the apical surface (Figure 1E). However, the rest of the cells exhibited rounded or spindly spreading shapes, with F-actin staining around the entire circumference and diffuse distribution of pEzrin, ZO-1, and Par1b (Figure 1, B and D). In this study cells with and without an F-actin cap colocalized with pEzrin are referred to as polarized and nonpolarized cells, respectively. Single IEC6 cells showed polarization in a time-dependent manner, and ~70% of cells were polarized at 4 h after seeding on Matrigel (Figure 1F). Time-lapse images showed that once cells are seeded on Matrigel, nonpolarized cells ruffled dynamically and
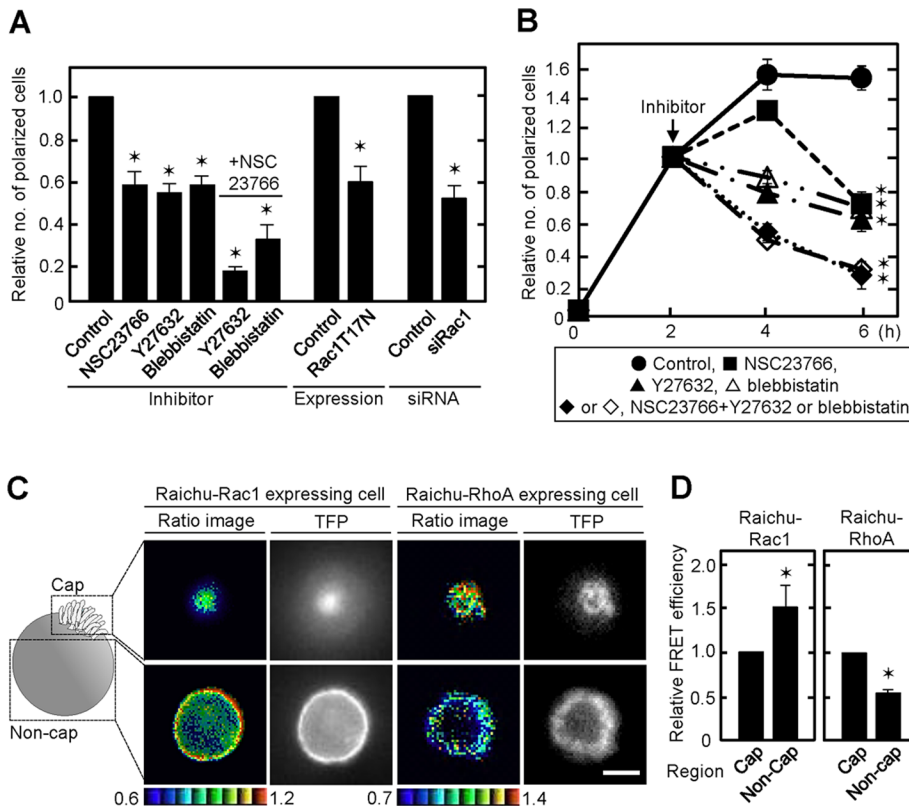
FIGURE 3: Spatially regulated Rac and Rho activities are involved in single-cell polarization. (A) IEC6 cells treated with NSC23766, Y27632, and/or blebbistatin and transiently transfected with GFP-Rac1T17N or transfected with Rac1 siRNA were plated on Matrigel for 2 h. Polarized cells among total cells were counted, and the percentage of polarized cells was calculated. The ratios of the percentages of polarized cells were compared with controls. (B) IEC6 cells were plated on Matrigel for 2 h and then further incubated for 2 or 4 h in presence of NSC23766 (■) and/or Y27632 (♦/▲) or blebbistatin (◊/△). ●, control. (C) IEC6 cells stably expressing Raichu-Rac1 or Raichu-RhoA were plated on Matrigel in a glass-bottomed dish for 2 h. Representative FRET/TFP ratio images are shown in the intensity-modulated display mode. The upper and lower limits of the ratio range are shown at the bottom. (D) Average of FRET/TFP ratio of representative cap or noncap areas in each FRET image of polarized IEC6 cells stably expressing Raichu-Rac1 ($n = 10$) or Raichu-RhoA ($n = 11$) was calculated to obtain FRET efficiency. Relative FRET efficiency in noncap areas was expressed compared with that in cap area. Results are shown as means ± SD from three independent experiments. *$p < 0.01$. Scale bar, 5 μm (C).

receptor for Wnt5a, reduced the number of polarized cells (Figure 2B and Supplemental Figure S2E). Dishevelled (Dvl), which consists of Dvl1, Dvl2, and Dvl3, is an important component of Wnt5a signaling (Wharton, 2003). When Dvl2 was depleted by siRNA against the coding region (siDvl2-1) and the 3'-untranslated region (siDvl2-2), single-cell polarization was suppressed (Figure 2B and Supplemental Figure S2F). Knockdown of Dvl1 or Dvl3 inhibited polarization to a lower extent than that of Dv2, and the polarity was further impaired by knockdown of all Dvls (Figure 2B and Supplemental Figure S2F). Expression of green fluorescent protein (GFP)–Dvl2 rescued the defect in single-cell polarization induced by siDvls-2 but not siDvls-1 (Figure 2D and Supplemental Figure S2F). Expression of GFP-Dvl2 rescued the defect in single-cell polarization induced by Wnt5a or Ror1 knockdown (Figure 2E and Supplemental Figure S2, D and E). Of note, Wnt5a- or GFP-Dvl2–expressing cells showed increased polarization compared with control cells (Figure 2, C–E). Collectively these gain- and loss-of-function experiments suggest that Wnt5a signaling is involved in the Matrigel-induced single-cell polarization through Ror1 and Dvl. Of importance, Wnt5a- or Dvls-depleted cells did not show polarized distribution of PKCζ and ZO-1

(Supplemental Figure S3), suggesting that Wnt5a signaling is involved in not only the formation of F-actin cap but also the establishment of AB polarity.

Rac and Rho activities are required for single-cell polarization

As shown in Figure 1, F-actin accumulated at the top of polarized cells, suggesting that the cytoskeleton is modulated dynamically. It is well known that small G proteins, Rac and Rho, regulate the cytoskeleton (Etienne-Manneville and Hall, 2002). After IEC6 cells were seeded on Matrigel, Rac1 was activated within 15 min and its activity maintained for 4 h (Supplemental Figure S4, A and B). RhoA activity in IEC6 cells was slightly elevated at 15 min after plating, followed by gradual inhibition (Supplemental Figure S4, A and B). When the cells were treated with NSC23766 (a Rac GEF inhibitor), Y27632 (a Rho kinase inhibitor), or blebbistatin (a myosin ATPase inhibitor), the ratio of polarized cells decreased (Figure 3A). The polarization was severely suppressed by simultaneous treatment with NSC23766 and Y27632 or blebbistatin (Figure 3A). In addition, expression of a dominant-negative form of Rac1 (Rac1T17N) or knockdown of Rac1 suppressed polarization (Figure 3A and Supplemental Figure S2G). The polarity at 6 h was also lost by treatment with NSC23766 and Y27632 or blebbistatin after single-cell polarization was established at 2 h (Figure 3B), suggesting that Rac1 and RhoA activities are necessary for the formation and maintenance of single-cell polarity.

To examine the spatial activation of Rac and Rho in single-cell polarization, we expressed Raichu-Rac1 and Raichu-RhoA, well-established fluorescence resonance energy transfer (FRET) probes, in IEC6 cells using recombinant retroviruses (Mochizuki et al., 2001; Yagi et al., 2012). The FRET/teal fluorescent protein (TFP) ratio was calculated to show FRET efficiency in polarized single cells, and the mosaic of ratio images was made up of pixels from blue to red, which corresponded to the lowest to the highest FRET efficiency (Figure 3C). Rac1 activity in the noncap region was higher than that in the cap region, whereas RhoA activity increased toward the cap region (Figure 3, C and D). Wnt5a- or Dvls-depleted IEC6 cells lost the polarity (Figure 2B). Therefore, Rac and Rho activities in the Matrigel-contacting (bottom) and Matrigel-noncontacting areas (top) were measured in these cells. There was no significant difference in Rac1 activity between Matrigel-contacting and -noncontacting areas, whereas RhoA activity decreased toward the noncontacting area (Supplemental Figure S4, C and D), supporting the idea that Wnt5a/Dvl signaling is involved in the polarized activation of Rac1 and RhoA. In addition, IEC6 cells cultured on type I collagen did not show the polarized activation of Rac1 and RhoA (Supplemental Figure S4, E and F). Thus, Rac1 and RhoA activities were spatially controlled, and their activation in different regions, which was regulated by Wnt5a signaling, was required for single-cell polarization.
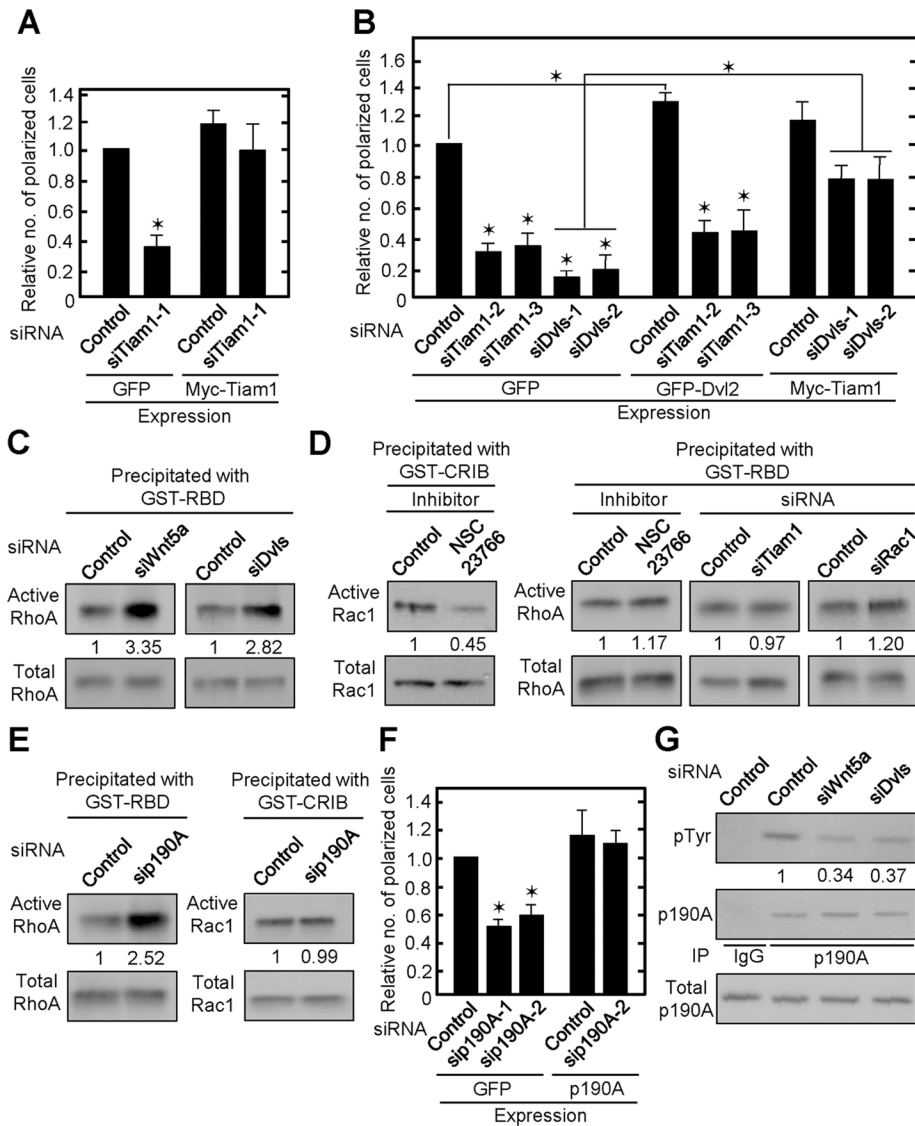
FIGURE 4: Wnt5a/Dvl signaling regulates Rac1 and RhoA activity through Tiam1 and p190RhoGAP-A on Matrigel. (A) IEC6 cells stably expressing GFP or Myc-Tiam1 were transfected with Tiam1-1 siRNA against 3′-untranslated region and plated on Matrigel for 2 h. Polarized cells among total cells were counted, and the percentage of polarized cells was calculated. The ratios of the percentages of polarized cells were compared with controls. (B) IEC6 cells stably expressing GFP, GFP-Dvl2, or Myc-Tiam1 were transfected with the indicated siRNAs and plated on Matrigel. SiTiam1-2 and -3 against the open reading frame. (C–E) Wnt5a- or Dvls-depleted (C), NSC23766-treated or Tiam1- or Rac1-depleted (D), or p190RhoGAP-A-depleted (E) IEC6 cells cultured on Matrigel for 1 h were lysed and subjected to RhoA (C, D, E) or Rac1 (D, E) assay, respectively. Fold changes of RhoA and Rac1 activities are shown as means from three independent experiments. CRIB, Cdc42/Rac interactive binding; GST, glutathione S-transferase; p190A, p190RhoGAP-A; RBD, Rho-binding domain. (F) p190RhoGAP-A-depleted-GFP or p190RhoGAP-A–expressing IEC6 cells were plated on Matrigel. Sip190A-1, against the open reading frame; p190A-2, against the 3′-untranslated region. The results are shown as means ± SD from three independent experiments. *$p < 0.01$. (G) Wnt5a- or Dvls-depleted IEC6 cells were plated on Matrigel for 2 h. The lysates were immunoprecipitated with anti-p190RhoGAP-A antibody, and the immunoprecipitates were probed with the indicated antibodies. Fold changes of p-Tyr levels by knockdown of Wnt5a or Dvls are shown as means from three independent experiments.

Wnt5a regulates Rac1 activity through Tiam1 on Matrigel

Wnt5a activated Rac1 in HeLaS3 and KKLS cells (Hanaki et al., 2012; Sato et al., 2010). Rac1 activity was indeed decreased in Wnt5a- or Dvls-depleted IEC6 cells cultured on Matrigel (Supplemental Figure S5A). We tested the involvement of Tiam1, which regulates Rac1 (Cajanek et al., 2013), in single-cell polarization. Knockdown of Tiam1 suppressed adhesion-dependent Rac1 activation (Supplemental Figure S5B). Single-cell polarization in Tiam1-depleted cells decreased, and expression of Myc-Tiam1 rescued cell polarity (Figure 4A and Supplemental Figure S2H). Expression of GFP-Dvl2 did not restore Rac1 activity or polarity in Tiam1-depleted cells, whereas expression of Myc-Tiam1 rescued Rac1 activity and partially restored polarity in Dvls-depleted cells (Figure 4B and Supplemental Figures S2, F and H, and S5B). FRET analyses revealed that the polarized distribution of Rac1 activity was disrupted by the knockdown of Tiam1 (Supplemental Figure S5, C and D), suggesting that Tiam1 is involved in the polarized activation of Rac1. These results suggest that Tiam1 functions downstream of Dvl in IEC6 cells and that Wnt5a signaling through Dvl and Tiam1 is involved in single-cell polarization of IEC6 cells.

Wnt5a regulates RhoA activity through p190RhoGAP-A on Matrigel

Although RhoA is activated in the β-catenin–independent pathway of various cells (Veeman et al., 2003; Schlessinger et al., 2009), knockdown of Wnt5a or Dvls activates RhoA in IEC6 cells (Figure 4C). Rac and Rho are regulated reciprocally in some cells; activation of Rac suppresses Rho and vice versa (Sanz-Moreno et al., 2008). However, under the condition in which Rac1 activity is inhibited by NSC23766 or siRNAs for Tiam1 and Rac1, RhoA activity is not changed (Figure 4D), implying that Wnt5a suppresses RhoA independently of the activation of Rac1. RhoA is negatively regulated by Rho GT-Pase-activating proteins (RhoGAPs; Tcherkezian and Lamarche-Vane, 2007). Among RhoGAPs, the activity of p190RhoGAP-A is regulated by focal adhesion kinase (FAK) and c-Src–mediated tyrosine phosphorylation in an adhesion-dependent manner (Chang et al., 1995; Tomar et al., 2009). In our culture conditions, RhoA activity increased in p190RhoGAP-A-depleted cells, although Rac1 activity was unchanged (Figure 4E and Supplemental Figure S2I). Knockdown of p190RhoGAP-A decreased single-cell polarization, and expression of p190RhoGAP-A restored the phenotype (Figure 4F and Supplemental Figure S2I).

p190RhoGAP-A was tyrosine phosphorylated 2 h after plating on Matrigel, and it was clearly reduced in Wnt5a- or Dvls-depleted IEC6 cells (Figure 4G). Consistent with our previous observations in HeLaS3 cells (Matsumoto et al., 2010), tyrosine phosphorylation of FAK at Y397 and paxillin at Y118, which are indicators of adhesion-dependent FAK activation, was also reduced in Wnt5a- or
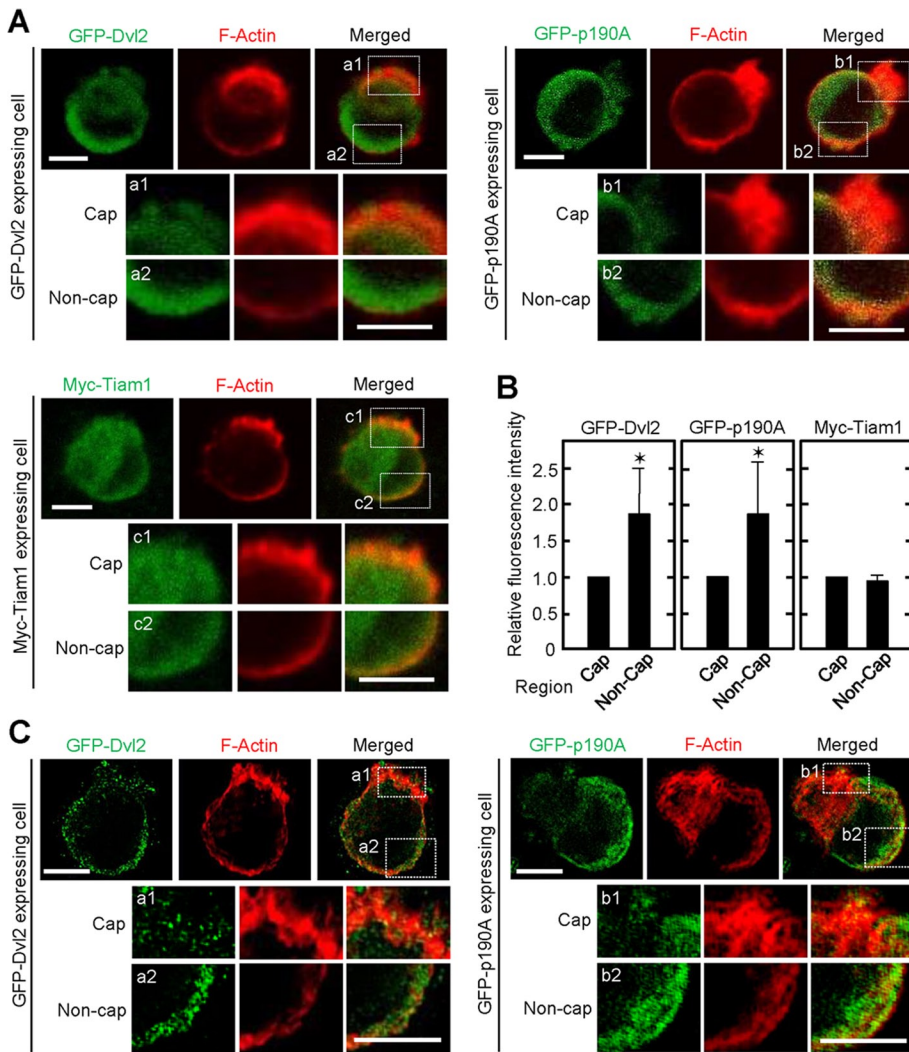
FIGURE 5: Localization of GFP-Dvl2, GFP-p190RhoGAP-A, and Myc-Tiam1. (A) IEC6 cells stably expressing GFP-Dvl2 (upper left), GFP-p190RhoGAP-A (upper right), or Myc-Tiam1 (bottom) were cultured on Matrigel for 2 h and stained for GFP (green) or Myc (green) and F-actin (red). The images are representative polarized cells. Bottom, enlarged image within dashed boxes (a1, a2, b1, b2, c1, and c2), indicating cap and noncap regions of polarized cells. (B) Average of fluorescence intensity in representative cap or noncap areas in polarized cells stably expressing GFP-Dvl2 ($n = 20$), GFP-p190RhoGAP-A ($n = 22$), or Myc-Tiam1 ($n = 22$) was measured, and the intensity in the noncap area was expressed relative to that in the cap area. The results are shown as means ± SD from three independent experiments. *$p < 0.01$. (C) Structured illumination microscopy demonstrates localization of GFP-Dvl2 (left) or GFP-p190RhoGAP-A (right) in polarized single IEC6 cells. Bottom, enlarged regions in the white boxes (a1, a2, b1, and b2). Scale bars, 5 μm (A, C).

mediates the adhesion signal (Figure 5, A and B). The localization of p190RhoGAP-A was predominantly in the noncap region of polarized single cells, which is consistent with the distribution of RhoA activity observed by FRET (Figure 5, A and B), whereas p190RhoGAP-A was distributed throughout the cell membrane and cytosol in Wnt5a- or Dvls-depleted cells (Supplemental Figure S6D). These results suggest that p190RhoGAP-A regulates Matrigel-adhesion-dependent RhoA activity properly by binding to Dvl in the basolateral membrane. On the other hand, Myc-Tiam1 was diffusely distributed (Figure 5, A and B). The polarized localization of GFP-Dvl2 and GFP-p190RhoGAP-A was confirmed by structured illumination microscopy (Figure 5C).

Dvl forms a complex with FAK, Tiam1, and p190RhoGAP-A

We then focused on identifying signaling mechanisms that might be modulated by Wnt5a/Dvl signaling. Consistent with our previous observations in HeLaS3 cells (Matsumoto et al., 2010), Dvl2 formed a complex with FAK in IEC6 cells at endogenous levels (Figure 6A). This complex formation was enhanced in Wnt5a-expressing cells and inhibited in Wnt5a-depleted cells (Figure 6, A and B), implying that Wnt5a signaling is involved in adhesion signaling through stabilization of the Dvl-FAK complex. The formation of a complex between Flag-Dvl2 and GFP-p190RhoGAP-A was observed in HEK293T cells (Figure 6C). Deletion mutant analyses revealed that p190RhoGAP-A binds to the C-terminal region of GFP-Dvl2 (506–736) or HA-Dvl1 (DEP+, 337–670) but not to GFP-Dvl2 (1–509) or HA-Dvl1 (1–398; Supplemental Figure S7, A and B).

Consistent with a recent report (Cajanek et al., 2013), HA-Dvl1 (1–398) and HA-Dvl1 (DEP+) formed a complex with Myc-Tiam1 (Supplemental Figure S7C). In addition, Myc-Tiam1 bound to both HA-Dvl1 (1–519) and HA-Dvl1 (DEP+), but GFP-p190RhoGAP-

Dvls-depleted cells (Supplemental Figure S6A). By the treatment with PF573228, a FAK inhibitor (Slack-Davis et al., 2007), single-cell polarization was decreased and RhoA but not Rac1 activity was elevated (Supplemental Figure S6, B and C), suggesting that FAK signal regulates RhoA predominantly through p190RhoGAP-A in polarized IEC6 cells in a Wnt5a/Dvl-dependent manner.

Spatial localization of Dvl, Tiam1, and p190RhoGAP-A in polarized IEC6 cells

To understand the role of Dvl, Tiam1, and p190RhoGAP-A in spatial regulation of Rac1 and RhoA activity, we investigated the localization of these key molecules in polarized IEC6 cells. Immunohistochemical analyses revealed that GFP-Dvl2 tends to be localized to the cell surface in contact with Matrigel, suggesting that Dvl

A associated only with HA-Dvl1 (DEP+), suggesting that Tiam1 and p190RhoGAP-A bind to different sites on Dvl (Supplemental Figure S7D). Indeed, expression of HA-Dvl1 (DEP+) enhanced the reciprocal formation of a complex between Tiam1 and p190RhoGAP-A (Figure 6D). In addition, complex formation between FAK, HA-Dvl2, Myc-Tiam1, and GFP-p190RhoGAP-A was observed in HEK293T cells (Figure 6E). The binding of p190RhoGAP-A to the C-terminal region of Dvl was important for the polarization of IEC6 cells because the expression of GFP-Dvl2 (1–509) neither enhanced single-cell polarization nor restored single-cell polarization in Dvls-depleted cells (Figure 6F and Supplemental Figure 2J). Taken together, these results suggest that Wnt5a promotes complex formation of FAK and Dvl, which binds to Tiam1 and p190RhoGAP-A simultaneously.
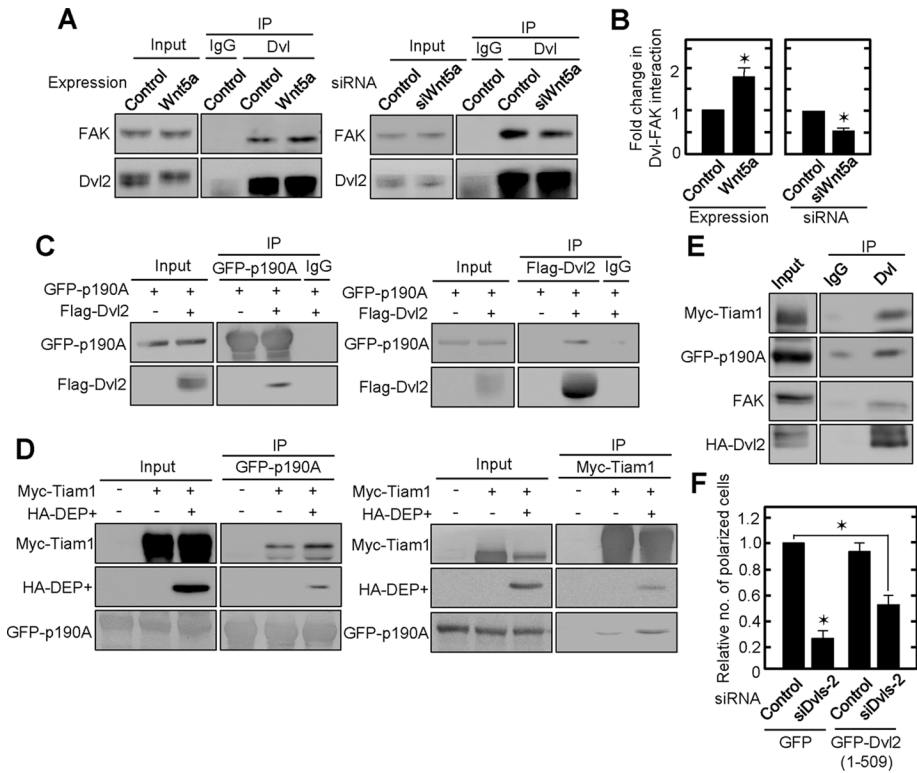
FIGURE 6: Complex formation between FAK, Dvl, Tiam1, and p190RhoGAP-A. (A) Lysates of Wnt5a-expressing or Wnt5a-depleted IEC6 cells cultured on Matrigel were immunoprecipitated with anti-Dvl (DIX) antibody. The immunoprecipitates were probed with anti-FAK and anti-Dvl2 antibodies. (B) The amounts of precipitated FAK and Dvl 2 shown in A were quantified by using Image J, and the ratio of the former to the latter was calculated. The ratios of the interaction of FAK and Dvl2 in Wnt5a-overexpressing or Wnt5a-depleted cells were expressed as fold changes compared with controls. (C) Flag-Dvl2 was expressed in HEK293T cells stably expressing GFP-p190RhoGAP-A, and the lysates were immunoprecipitated with anti-GFP or anti-Flag antibody. The immunoprecipitates were probed with anti-GFP and anti-Flag antibodies. (D) Myc-Tiam1 and/or HA-Dvl1 (DEP+) were expressed in HEK293T cells stably expressing GFP-p190RhoGAP-A, and the lysates were immunoprecipitated with anti-GFP or anti-Myc antibody. The immunoprecipitates were probed with anti-Myc, anti-hemagglutinin (HA), and anti-GFP antibodies. (E) Myc-Tiam1 and HA-Dvl2 were expressed in HEK293T cells stably expressing GFP-p190RhoGAP-A, and the lysates were immunoprecipitated with anti-Dvl (DIX) antibody. The immunoprecipitates were probed with anti-Myc, anti-GFP, anti-FAK, and anti-HA antibodies. (F) GFP or GFP-Dvl2 deletion mutant (1–509)–expressing IEC6 cells transfected with siDvls-2 siRNA were plated on Matrigel. Polarized cells among total cells were counted, and the percentage of polarized cells was calculated. The ratios of the percentages of polarized cells were compared with controls. Results are shown as means ± SD from three independent experiments. *$p < 0.01$.

Wnt5a signaling is required for cyst formation of IEC6 cells

Finally, we tested whether single-cell polarization reflects AB polarization formed by multiple epithelial cells. IEC6 cells formed cysts, spherical monolayer of cells that enclose apical lumens, where F-actin and pEzrin accumulated when the cells were cultured in Matrigel three-dimensionally for 72 h (Figure 7A). The apical membrane was fragmented by treatment with either Y27632 or PF573228, suggesting that the appropriate level of RhoA activity was important for the formation of apical structures (Figure 7, A and B). Continuous but expanded and distorted lumens and partially disrupted basolateral membranes were observed in IEC6 cysts after treatment with NSC23766 (Figure 7, A and B). Therefore Rac1 might be involved in the integrity of the basolateral membrane in IEC6 cysts, leading to the apical structure to be centralized and circular. Indeed, basolateral membranes of NSC23766- but not Y27632- or PF573228-treated cysts were partially collapsed, according to the assessment

of intensity line scans of basolateral membranes stained using an anti–β-catenin antibody (Supplemental Figure S8). When IEC6 cysts were treated with NSC23766 and Y27632 or PF573228 simultaneously, they lost lumen integrity, with fragmented apical and disrupted basolateral structures, which are believed to be a combination of phenotypes induced by their single treatment (Figure 7, A and B). Wnt5a- or Dvls-depleted IEC6 cysts exhibited similar phenotypes (Figure 7, C and D). Thus balanced control between Rac and Rho mediated by Wnt5a/Dvl signal could be important for lumen formation consisting of multiple IEC6 cells, as well as for single-cell polarization.

DISCUSSION

Wnt5a signaling is involved in single-cell polarization

Here we showed that Wnt5a signaling is involved in Matrigel-adhesion-dependent AB polarization of single IEC6 cells. EpH4 and MDCK cells did not show a spherical shape with an F-actin cap, and the expression level of Wnt5a in these cells was lower than that in IEC6 cells. These results do not always reflect that low Wnt5a signal activity is the reason for failure of single-cell polarization of EpH4 and MDCK cells. Thus, although this process might be unique in IEC6 cells, the results suggest that normal epithelial cells have the potential to develop AB polarity without cell-to-cell adhesion.

Wnt5a is expressed in the mesoderm of caudal primitive streaks, mesenchyme of gut, limb, and outer ears at various stages of developmental processes (Yamaguchi et al., 1999) and is also expressed in the epithelium of the urogenital sinus, hindgut, and cloacal membrane and in uterine lumenal epithelial cells (Daikoku et al., 2011; Li et al., 2011). In adults, Wnt5a is rarely found in normal tissues but is expressed in inflammatory cells or cancer cells (Veeman et al., 2003; Kikuchi et al., 2012). Therefore, IEC6 cells are a good model with which to analyze the functions of Wnt5a when it is released from normal epithelial cells.

Evidence has accumulated that Wnt signaling, especially the β-catenin–dependent pathway, affects AB polarity. In *Drosophila* and *Xenopus*, Dvl binds to Lgl, which is required for the formation of cell polarity and regulates its stability and basolateral localization (Dollar et al., 2005). Overexpression of Fz8 sequesters Dvl from Lgl, resulting in the loss of membrane localization. Tiam1 and fibronectin, which are associated with the AB polarity protein Par-3 and are essential for the establishment of AB polarity, are direct transcriptional targets of Wnt signaling (Gradl et al., 1999; Malliri et al., 2006). As to the β-catenin–independent pathway, Wnt5a-knockout mice show disruption of intestinal epithelial structure by epithelial clumps where the apical distribution of atypical PKC and subcellular distribution of Fz3 and Dvl2 are disturbed (Matsuyama et al., 2009). However, these findings are restricted to the formation of AB polarity
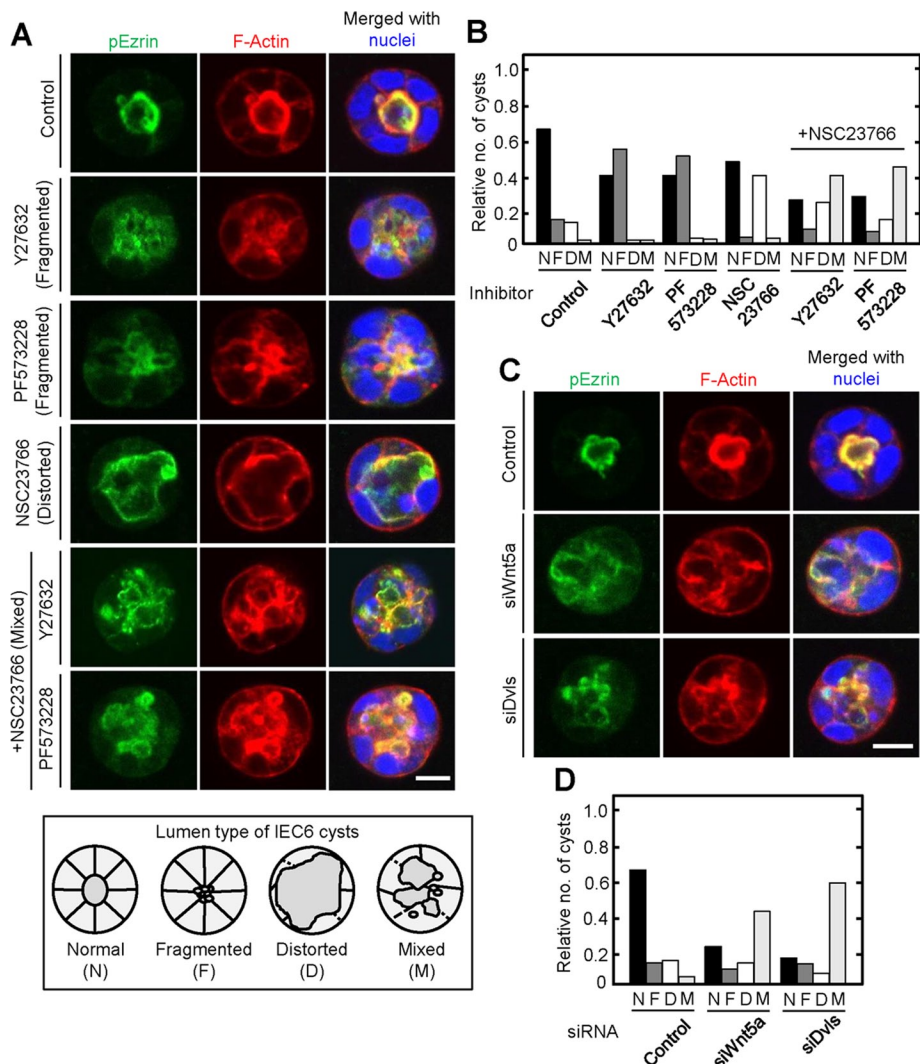
FIGURE 7: Wnt5a signaling is involved in lumen formation of IEC6 cysts. (A) Top, IEC6 cells treated with Y27632, PF573228, and/or NSC23766 were plated on Matrigel for 72 h and then stained for pEzrin (green), F-actin (red), and DRAQ5 (blue). Bottom, schematic images of IEC6 cysts with normal (N), fragmented (F), distorted (D), or mixed (fragmented and distorted; M) lumens. (B) IEC6 cysts treated with the indicated inhibitors were classified by their lumenal patterns, and the relative cyst numbers among the different patterns in each treatment were expressed. (C) Wnt5a- or Dvls-depleted IEC6 cells were plated on Matrigel for 72 h and stained for pEzrin (green), F-actin (red), and DRAQ5 (blue). Scale bars, 10 μm. (D) Wnt5a- or Dvls-depleted IEC6 cells were cultured on Matrigel for 72 h, and the cysts were classified by their lumenal pattern. The results shown are means from three independent experiments. Scale bar, 10 μm (A, C).

that requires cell-to-cell adhesion. Our results clearly showed that Wnt5a signaling promotes Matrigel-dependent orientation of AB polarity at single-cell levels in the absence of cell-to-cell junction. Because Matrigel but not type I collagen induced single-cell polarization, specific ECM proteins could play important roles in the cooperative functions of Wnt5a and integrin signaling.

Spatial regulation of Rac and Rho activities is essential for single-cell polarization

We found that Rac1 and RhoA are activated at the basolateral and apical membranes, respectively, and these activities are necessary for the formation of single-cell polarization. In addition, as treatment with inhibitors of Rac and Rho kinase after F-actin cap formation disrupts the cap structure, Rac1 and RhoA activities seem to be

required not only for establishment but also for maintenance of the cap structure. Although Wnt5a activates Rac1 in various cell lines (Kurayoshi et al., 2006; Sato et al., 2010), its mechanism was poorly understood. While this article was being prepared, a report appeared showing that Tiam1 is required for Wnt5a- and Dvl-induced activation of Rac1 in HEK293T cells and dopaminergic neuronal cells (Cajanek et al., 2013). Consistent with these results, Tiam1 bound to the C-terminal region of Dvl and acted downstream of Dvl in the orientation of AB polarity.

Rho is an important component of the β-catenin–independent pathway, especially in *Drosophila* and *Xenopus* (Kikuchi et al., 2012; Veeman et al., 2003). However, the relationship between Wnt5a and Rho is not clear, except that Wnt5a induces osteogenic differentiation in mesenchymal stromal cells through the activation of Rho kinase (Santos et al., 2010). Our results showed that Wnt5a signaling inhibits RhoA through p190RhoGAP-A. However, because treatment with Y27632 disturbed single-cell polarization, RhoA activity must be maintained appropriately. Therefore it is important that Wnt signaling decreased Rho activity spatially and temporarily. Furthermore, Wnt5a and Dvls were required for tyrosine phosphorylation of p190RhoGAP-A, which is necessary for adhesion-dependent RhoGAP activity. FAK is a major player in the tyrosine phosphorylation of p190RhoGAP-A (Chikumi et al., 2004; Holinstat et al., 2006; Tomar et al., 2009). In our study, RhoA activity was elevated by the inhibition of FAK, suggesting that the activation of FAK might suppress RhoA activity through p190RhoGAP-A rather than RhoGEFs.

A signaling complex including FAK, Dvl, Tiam1, and p190RhoGAP-A regulates adhesion-dependent apical and basolateral polarization of IEC6 cells

Dvl formed a complex with FAK in a Wnt5a-dependent manner, and Wnt5a and Dvl were required for the activation of FAK in IEC6 cells. In addition, Dvl, Tiam1, and p190RhoGAP-A formed a tertiary complex. Therefore it is intriguing to speculate that Dvl is recruited to the cell membranes where FAK is present and associates with Tiam1 and p190RhoGAP-A. Rac1 activity was elevated through Tiam1, and RhoA activity was properly suppressed by p190RhoGAP-A, which might be tyrosine phosphorylated through FAK and activated. Therefore Wnt5a signaling could modulate Rac and Rho activities through interaction of their regulators with Dvl and FAK.

How does Wnt5a regulate Rac and Rho spatially? Dvl and p190RhoGAP-A were localized to the noncap region predominantly compared with the cap region, consistent with the distribution of RhoA activity observed by FRET. Although Tiam1 was observed in both cap and noncap regions equally, Tiam1 activity might be higher

by binding to Dvl at the noncap region. Alternatively, Rac activity might be modulated in the cap region by unknown mechanisms such as the localization of Rac GAP. In addition, we showed previously that Fz2, a Wnt5a receptor, forms a complex with integrin α2 and that Wnt5a and Dvls promote cell-to-substrate adhesion (Matsumoto et al., 2010). Taking these results together, we propose the following model. When epithelial cells bind to basement membrane proteins, integrin/FAK signaling is activated. Fz, which localized to integrin closely, is activated by Wnt5a, and Fz and integrin recruit the Dvl/FAK complex. Tiam1 and p190RhoGAP-A, which are associated with Dvl, activate Rac and inhibit Rho, respectively, spatially in regions surrounded by basement membranes. Spatial regulation of Rac and Rho polarizes their activities, which orients cell polarization (Supplemental Figure S9).

Rac and Rho activities were necessary for AB polarization of MDCK cells in three-dimensional culture (O'Brien et al., 2001; Yu et al., 2008). The FRET system revealed that in the process of cystogenesis, polarity of Rac1 activity was not observed in the early stage and was activated at the basolateral membrane in the later stage (Yagi et al., 2012). In contrast, RhoA activity was higher at the apical membrane in the early stage, but its polarized activity was lost in the later stage. In cysts consisting of multiple IEC6 cells, inhibition or activation of Rho induced the fragmentation of the apical lumen, whereas inhibition of Rac mainly damaged the basolateral membrane. These may reflect localized activation of Rac1 in the basal region and RhoA in the apical region of IEC6 cysts, as in polarized cells at the single-cell level. Thus there might be common mechanisms in the formation of AB polarization between single epithelial cells and cysts.

MATERIALS AND METHODS

pCX4neoDX/Raichu-Rac1 and pCX4neoDX/Raichu-RhoA, pCS2/FLAG-Dvl2, pCSMT/Myc-Tiam1, p3×Flag-CMV10/p190RhoGAP-A, LifeAct-mCherry, pAcGFP/PLCδ1-PH, pEGFP/actin, and anti-Par1b antibody were kindly provided by M. Matsuda (Kyoto University, Kyoto, Japan), R. Habas (Robert Wood Johnson Medical School, University of Medicine and Dentistry of New Jersey, Piscataway, NJ), H. Sugimura (Hamamatsu University School of Medicine, Shizuoka, Japan), N. Mochizuki (National Cerebral and Cardiovascular Center Research Institute, Osaka, Japan), K. Ohashi (Tohoku University, Miyagi, Japan), Y. Irino (Kobe University, Hyogo, Japan), K. Kaibuchi (Nagoya University Graduate School of Medicine, Aichi, Japan), and S. Ohno (Yokohama City University School of Medicine, Kanagawa, Japan), respectively.

pPGK-neo/Wnt5a and pCGN/Dvl1 or pEGFPC1/Dvl2 deletion mutants used in this study were constructed as described previously (Kishida et al., 1999, 2001; Hino et al., 2001, 2003; Matsumoto et al., 2010; Fumoto et al., 2012). Standard recombinant DNA techniques were used to construct pEGFPC1/Rac1^{T17N} and pEGFPC3/p190RhoGAP-A.

To construct lentiviral vectors, GFP, Wnt5a, and GFP-Dvl2 cDNAs were cloned into pLvSIN (Takara Bio, Shiga, Japan) and Myc-Tiam1, p190RhoGAP-A, GFP-p190RhoGAP-A, GFP-Dvl2 (1-509), and GFP-PLCδ1-PH cDNAs were cloned into CSII-CMV-MCS-IRES2-Bsd (RIKEN BioResource Center, Ibaraki, Japan). The lentiviruses were produced as described previously (Fumoto et al., 2012). The retroviruses were produced in HEK293P cells by expressing Raichu-Rac1 or Raichu-RhoA using Lipofectamine 2000 (Life Technologies, Tokyo, Japan).

All of the primary antibodies used in this study are listed in Supplemental Table S1. An anti-Dvl1 (DIX) antibody was generated as described previously (Sakamoto et al., 2000). The anti-Myc antibody was prepared from 9E10 cells. The RNA duplexes used for siRNA experiments are shown in Supplemental Table S2. Forward and reverse primers used for quantitative real-time PCR are shown in Supplemental Table S3.

Cell culture and transfection

IEC6 cells were maintained in α-MEM containing 10% fetal bovine serum (FBS), 10 μg/ml insulin, 4.5 mg/ml glucose, and 1× nonessential amino acids. HEK293T cells were maintained in DMEM/Ham's F12 (1:1) supplemented with 10% FBS. X293T, HEK293P, EpH4, and MDCK cells were maintained in DMEM supplemented with 10% FBS.

IEC6 cells stably expressing GFP, Wnt5a, GFP-Dvl2, Raichu-Rac1, Raichu-RhoA, Myc-Tiam1, p190RhoGAP-A, GFP-p190RhoGAP-A, GFP-Dvl2 (1-509), or GFP-PLCδ1-PH and HEK293T cells stably expressing Myc-Tiam1, p190RhoGAP-A, or GFP-p190RhoGAP-A were generated as described previously (Fumoto et al., 2012). The cells treated with lentiviruses or retroviruses were selected and maintained in the parental cell culture medium with 400 μg/ml G418 or 2.5 μg/ml blasticidin S. IEC6 cells stably expressing Raichu-Rac1 or Raichu-RhoA were collected by fluorescence-activated cell sorting to select highly expressing cells. To express proteins transiently, IEC6 and HEK293T cells were transfected with plasmids using Fu-GENE HD and Lipofectamine 2000, respectively.

Single-cell and cyst culture on thick Matrigel

We spread 40 μl of Matrigel (BD Biosciences, Tokyo, Japan) or collagen type I (KOKEN, Tokyo, Japan) on a round coverslip (15-mm diameter) and incubated at 37°C for 20 or 30 min to solidify the gel, respectively. IEC6 cells were trypsinized to a single-cell suspension at 3×10^4 cells/ml in growth medium containing 2% Matrigel (vol/vol), seeded on solidified thick gel, and then incubated for 2 h. For cyst formation of IEC6 cells, cell suspension (5×10^4 cells/ml) containing 2% Matrigel (vol/vol) and epidermal growth factor (0.2 ng/ml) was seeded on solidified Matrigel, and further incubation was performed for 72 h. For treatment with inhibitors, 0.5 μM Y27632 (Wako, Osaka, Japan) or 0.5 μM blebbistatin (Toronto Research Chemicals, Toronto, Canada) was added when plating on Matrigel. When 10 μM IWP2 (Wako), 10 μM IWR1 (Sigma Aldrich, Tokyo, Japan), 100 μM NSC23766 (Merck Millipore, Tokyo, Japan), or 0.5 μM PF573228 (Merck Millipore) was used, IEC6 cells were pretreated with the indicated reagents before assays (for 24 h with IWP2 and IWR1, for 12 h with NSC23766, and for 4 h with PF573228), and single-cell culture was performed in growth medium including the same concentrations of reagents.

Immunocytochemistry

Cells grown on Matrigel-coated glass coverslips were fixed for 15 min at room temperature in phosphate-buffered saline (PBS) containing 4% (wt/vol) paraformaldehyde and permeabilized with PBS containing 0.1% (wt/vol) Triton X-100. The cells were then washed three times with PBS and blocked for 30 min with 0.5% BSA in PBS. The subsequent procedures were performed as described previously (Fumoto et al., 2012). When necessary, nuclei were stained with DRAQ5 (1:1000; BioStatus Limited, Shepshed, United Kingdom).

Electron microscopy

To perform SEM, the cells were fixed in 2.5% glutaraldehyde in phosphate buffer 0.1 M (pH 7.4) at 4°C for 2 h and postfixed in 1% OsO4 solution at 4°C for 1 h. After fixation, the cells were dehydrated in graded concentrations of ethanol and dried naturally in a desiccator. Finally, samples were coated with osmium using an

osmium plasma coater (Meiwafosis, Tokyo, Japan). Observations were performed using a scanning electron microscope (S-4800; Hitachi, Tokyo, Japan). For TEM, cells were fixed with 2.5% glutaraldehyde in phosphate buffer 0.1 M (pH 7.4) at 4°C for 2 h, postfixed in 1% OsO_4 solution at 4°C for 1 h, dehydrated in graded concentrations of ethanol, and embedded in epoxy resin (Quetol 812; Nissin EM, Tokyo, Japan). Ultrathin sections (80 nm) cut using an ultramicrotome (Ultracut E; Reichert, Depew, NY) were stained with uranyl acetate and lead citrate and examined with a transmission electron microscope (Hitachi H-7650) at 80 kV.

FRET imaging
IEC6 cells stably expressing Raichu-Rac1 or Raichu-RhoA (Yagi et al., 2012) were plated on solidified Matrigel in glass-bottomed dishes and cultured for 2 h. The cells were examined using an IX81-ZDC microscope (Olympus, Tokyo, Japan) equipped with a cooled charge-coupled device camera (CoolSNAP HQ; Roper Scientific, Tucson, AZ), and an MD-XY30100T-Meta automatically programmable XY stage (SIGMA KOKI, Tokyo, Japan). After background subtraction, FRET/TFP ratio images were created using MetaMorph software (Universal Imaging, West Chester, PA), and represented by intensity display mode (IMD). In the IMD mode, eight colors from red to blue are used to represent the FRET/TFP ratios. For each image, the average of ratio images of representative apical or basal areas was measured on FRET efficiency maps. Normalizations were carried out by dividing values obtained from noncap areas by the values obtained from cap areas.

Rac and Rho activation assay
After serum starvation for 12 h, IEC6 cells were detached and kept in suspension in medium containing 0.2% BSA for 45 min. Cells (1 × 10^6) were seeded on solidified Matrigel (10-cm-diameter dish) and incubated for the indicated periods at 37°C. Rac and Rho activities were assayed as described previously (Kishida et al., 2004; Sato et al., 2010)

Statistical analysis
The experiments were performed at least three times, and the results are expressed as means or means ± SD. Statistical analysis was performed using the paired Student's t test. For the quantification of polarized cells, at least 100 cells or 30 plasmid-transfected cells were counted per experiment. For the quantification of polarized cysts, at least 50 cysts were counted per experiment. Protein expression levels were quantified by densitometry analysis using ImageJ software (National Institutes of Health, Bethesda, MD), and the signals are expressed as arbitrary units compared with the signal intensity in control cells. $p < 0.01$ was considered statistically significant.

Other methods
Methods for immunoblotting, immunoprecipitation, transfection of siRNA, and quantitative real-time PCR were described previously (Matsumoto et al., 2010; Sato et al., 2010).

REFERENCES
Baas AF, Kuipers J, van der Wel NN, Batlle E, Koerten HK, Peters PJ, Clevers HC (2004). Complete polarization of single intestinal epithelial cells upon activation of LKB1 by STRAD. Cell 116, 457–466.

Baum B, Georgiou M (2011). Dynamics of adherens junctions in epithelial establishment, maintenance, and remodeling. J Cell Biol 192, 907–917.

Berzat A, Hall A (2010). Cellular responses to extracellular guidance cues. EMBO J 29, 2734–2745.

Bryant DM, Mostov KE (2008). From cells to organs: building polarized tissue. Nat Rev Mol Cell Biol 9, 887–901.

Cajanek L, Ganji RS, Henriques-Oliveira C, Theofilopoulos S, Konik P, Bryja V, Arenas E (2013). Tiam1 regulates the Wnt/Dvl/Rac1 signaling pathway and the differentiation of midbrain dopaminergic neurons. Mol Cell Biol 33, 59–70.

Chang JH, Gill S, Settleman J, Parsons SJ (1995). c-Src regulates the simultaneous rearrangement of actin cytoskeleton, p190RhoGAP, and p120RasGAP following epidermal growth factor stimulation. J Cell Biol 130, 355–368.

Chen B et al. (2009). Small molecule-mediated disruption of Wnt-dependent signaling in tissue regeneration and cancer. Nat Chem Biol 5, 100–107.

Chikumi H, Barac A, Behbahani B, Gao Y, Teramoto H, Zheng Y, Gutkind JS (2004). Homo- and hetero-oligomerization of PDZ-RhoGEF, LARG and p115RhoGEF by their C-terminal region regulates their in vivo Rho GEF activity and transforming potential. Oncogene 23, 233–240.

Daikoku T et al. (2011). Conditional deletion of Msx homeobox genes in the uterus inhibits blastocyst implantation by altering uterine receptivity. Dev Cell 21, 1014–1025.

Dollar GL, Weber U, Mlodzik M, Sokol SY (2005). Regulation of Lethal giant larvae by Dishevelled. Nature 437, 1376–1380.

Etienne-Manneville S, Hall A (2002). Rho GTPases in cell biology. Nature 420, 629–635.

Fumoto K, Kikuchi K, Gon H, Kikuchi A (2012). Wnt5a signaling controls cytokinesis by correctly positioning ESCRT-III at the midbody. J Cell Sci 125, 4822–4832.

Gloerich M, ten Klooster JP, Vliem MJ, Koorman T, Zwartkruis FJ, Clevers H, Bos JL (2012). Rap2A links intestinal cell polarity to brush border formation. Nat Cell Biol 14, 793–801.

Gradl D, Kuhl M, Wedlich D (1999). The Wnt/Wg signal transducer β-catenin controls fibronectin expression. Mol Cell Biol 19, 5576–5587.

Grindstaff KK, Yeaman C, Anandasabapathy N, Hsu SC, Rodriguez-Boulan E, Scheller RH, Nelson WJ (1998). Sec6/8 complex is recruited to cell-cell contacts and specifies transport vesicle delivery to the basal-lateral membrane in epithelial cells. Cell 93, 731–740.

Hanaki H, Yamamoto H, Sakane H, Matsumoto S, Ohdan H, Sato A, Kikuchi A (2012). An anti-Wnt5a antibody suppresses metastasis of gastric cancer cells in vivo by inhibiting receptor-mediated endocytosis. Mol Cancer Ther 11, 298–307.

Hino S, Kishida S, Michiue T, Fukui A, Sakamoto I, Takada S, Asashima M, Kikuchi A (2001). Inhibition of the Wnt signaling pathway by Idax, a novel Dvl-binding protein. Mol Cell Biol 21, 330–342.

Hino S, Michiue T, Asashima M, Kikuchi A (2003). Casein kinase 1ε enhances the binding of Dvl-1 to Frat-1 and is essential for Wnt-3a-induced accumulation of β-catenin. J Biol Chem 278, 14066–14073.

Holinstat M, Knezevic N, Broman M, Samarel AM, Malik AB, Mehta D (2006). Suppression of RhoA activity by focal adhesion kinase-induced activation of p190RhoGAP: role in regulation of endothelial permeability. J Biol Chem 281, 2296–2305.

Kikuchi A, Yamamoto H, Sato A, Matsumoto S (2011). New insights into the mechanism of wnt signaling pathway activation. Int Rev Cell Mol Biol 291, 21–71.

Kikuchi A, Yamamoto H, Sato A, Matsumoto S (2012). Wnt5a: its signalling, functions and implication in diseases. Acta Physiol (Oxf) 204, 17–33.

Kishida M, Hino SI, Michiue T, Yamamoto H, Kishida S, Fukui A, Asashima M, Kikuchi A (2001). Synergistic activation of the Wnt signaling pathway by Dvl and casein kinase Iε. J Biol Chem 276, 33147–33155.

Kishida S, Yamamoto H, Hino SI, Ikeda S, Kishida M, Kikuchi A (1999). DIX domains of Dvl and axin are necessary for protein interactions and their ability to regulate β-catenin stability. Mol Cell Biol 19, 4414–4422.

Kishida S, Yamamoto H, Kikuchi A (2004). Wnt-3a and Dvl induce neurite retraction by activating Rho-associated kinase. Mol Cell Biol 24, 4487–4501.

Kurayoshi M, Oue N, Yamamoto H, Kishida M, Inoue A, Asahara T, Yasui W, Kikuchi A (2006). Expression of Wnt-5a is correlated with aggressiveness of gastric cancer by stimulating cell migration and invasion. Cancer Res 66, 10439–10448.

Li FF, Zhang T, Bai YZ, Yuan ZW, Wang WL (2011). Spatiotemporal expression of Wnt5a during the development of the hindgut and anorectum in human embryos. Int J Colorectal Dis 26, 983–988.

Logan CY, Nusse R (2004). The Wnt signaling pathway in development and disease. Annu Rev Cell Dev Biol 20, 781–810.

Malliri A, Rygiel TP, van der Kammen RA, Song JY, Engers R, Hurlstone AF, Clevers H, Collard JG (2006). The rac activator Tiam1 is a Wnt-responsive gene that modifies intestinal tumor development. J Biol Chem 281, 543–548.

Matsumoto S, Fumoto K, Okamoto T, Kaibuchi K, Kikuchi A (2010). Binding of APC and Dishevelled mediates Wnt5a-regulated focal adhesion dynamics in migrating cells. EMBO J 29, 1192–1204.

Matsuyama M, Aizawa S, Shimono A (2009). Sfrp controls apicobasal polarity and oriented cell division in developing gut epithelium. PLoS Genet 5, e1000427.

Mochizuki N, Yamashita S, Kurokawa K, Ohba Y, Nagai T, Miyawaki A, Matsuda M (2001). Spatio-temporal images of growth-factor-induced activation of Ras and Rap1. Nature 411, 1065–1068.

O'Brien LE, Jou TS, Pollack AL, Zhang Q, Hansen SH, Yurchenco P, Mostov KE (2001). Rac1 orientates epithelial apical polarity through effects on basolateral laminin assembly. Nat Cell Biol 3, 831–838.

Sakamoto I et al. (2000). A novel β-catenin-binding protein inhibits β-catenin-dependent Tcf activation and axis formation. J Biol Chem 275, 32871–32878.

Santos A, Bakker AD, de Blieck-Hogervorst JM, Klein-Nulend J (2010). WNT5A induces osteogenic differentiation of human adipose stem cells via rho-associated kinase ROCK. Cytotherapy 12, 924–932.

Sanz-Moreno V, Gadea G, Ahn J, Paterson H, Marra P, Pinner S, Sahai E, Marshall CJ (2008). Rac activation and inactivation control plasticity of tumor cell movement. Cell 135, 510–523.

Sato A, Yamamoto H, Sakane H, Koyama H, Kikuchi A (2010). Wnt5a regulates distinct signalling pathways by binding to Frizzled2. EMBO J 29, 41–54.

Schlessinger K, Hall A, Tolwinski N (2009). Wnt signaling pathways meet Rho GTPases. Genes Dev 23, 265–277.

Slack-Davis JK et al. (2007). Cellular characterization of a novel focal adhesion kinase inhibitor. J Biol Chem 282, 14845–14852.

Suzuki A, Ishiyama C, Hashiba K, Shimizu M, Ebnet K, Ohno S (2002). aPKC kinase activity is required for the asymmetric differentiation of the premature junctional complex during epithelial cell polarization. J Cell Sci 115, 3565–3573.

Tcherkezian J, Lamarche-Vane N (2007). Current knowledge of the large RhoGAP family of proteins. Biol Cell 99, 67–86.

Tomar A, Lim ST, Lim Y, Schlaepfer DD (2009). A FAK-p120RasGAP-p190RhoGAP complex regulates polarity in migrating cells. J Cell Sci 122, 1852–1862.

Umeda K, Ikenouchi J, Katahira-Tayama S, Furuse K, Sasaki H, Nakayama M, Matsui T, Tsukita S, Furuse M (2006). ZO-1 and ZO-2 independently determine where claudins are polymerized in tight-junction strand formation. Cell 126, 741–754.

Veeman MT, Axelrod JD, Moon RT (2003). A second canon. Functions and mechanisms of β-catenin-independent Wnt signaling. Dev Cell 5, 367–377.

Vega-Salas DE, Salas PJ, Gundersen D, Rodriguez-Boulan E (1987). Formation of the apical pole of epithelial (Madin-Darby canine kidney) cells: polarity of an apical protein is independent of tight junctions while segregation of a basolateral marker requires cell-cell interactions. J Cell Biol 104, 905–916.

Wharton KAJ (2003). Runnin' with the Dvl: proteins that associate with Dsh/Dvl and their significance to Wnt signal transduction. Dev Biol 253, 1–17.

Yagi S, Matsuda M, Kiyokawa E (2012). Suppression of Rac1 activity at the apical membrane of MDCK cells is essential for cyst structure maintenance. EMBO Rep 13, 237–243.

Yamaguchi TP, Bradley A, McMahon AP, Jones S (1999). A Wnt5a pathway underlies outgrowth of multiple structures in the vertebrate embryo. Development 126, 1211–1223.

Yamamoto H, Kitadai Y, Yamamoto H, Oue N, Ohdan H, Yasui W, Kikuchi A (2009). Laminin γ2 mediates Wnt5a-induced invasion of gastric cancer cells. Gastroenterology 137, 242–252.

Yu W et al. (2008). Involvement of RhoA, ROCK I and myosin II in inverted orientation of epithelial polarity. EMBO Rep 9, 923–929.